

Experimental Studies on Bluff Bodies

V. Siva Kanna¹, P.Bhagyasri², A. Rama Krishna³P.G. Student, Department of Mechanical Engineering, BVC Engineering College, Odalarevu, A.P, India¹Assistant Professor, Department of Mechanical Engineering, VVIT, Nambur, A.P, India²Professor, Department of Mechanical Engineering, BVC Engineering College, Odalarevu, A.P, India³

ABSTRACT: This paper presents the experimental studies on Bluff bodies. In the present study a blunt nosed body with and without spike having the $L/W = 1$ and 1.5 , where W is the width of the model and L is the length of the spike are chosen. The zone of influence and the positive pressure field over the nose for a blunt-nosed body, with and without spike were measured by direct means. Flow past the body, with and without spikes was visualized in a two dimensional water channel at a Reynolds number 6620. It is found that the spike reduces the radius of curvature of the approaching streamline, and the deflection of the streamline is towards the shoulder of the basic body resulting in a narrow zone of positive pressure hill at the nose. The spike with hemispherical nose reduces the zone of influence.

KEYWORDS: Aerodynamics, blunt- nosed body, Vortex, aero-spike, visualization

I. INTRODUCTION

The drag reduction of a blunt-nosed body plays an important role in low- speed and high-speed applications. This assumes a lot of importance in the case of hypersonic flying objects because of the extremely high drag caused by the high-pressure zone at the nose, owing to the blunt nature of the geometry. But the blunt shape is essential for the nose of the hypersonic vehicles to safeguard the body from ablation caused by aerodynamic heating. For reducing the drag, secondary objects projecting ahead of the blunt nose has been found to be an effective method. These secondary objects are termed spikes, in general. When a spike is fixed to a blunt nose, it essentially shifts the forward stagnation point away from the surface of the blunt nose, as shown in Figure 1. Because of this, the extent of the positive pressure zone over the blunt nose comes down, leading to reduced drag. The flow process associated with the shifting of the stagnation point upstream of the blunt nose would results in weakening of the detached shock, and reduction of the extent of the zone influenced by the detached shock. Several experimental studies have been conducted to examine the fore body flow field of the spiked blunt body. The present work is an attempt in this direction to measure the zone of influence, and the positive pressure field over the nose of a blunt-nosed body, with and without spike, by direct means. For this, flow past the desired blunt-nosed body, with without spikes, was visualized in a simple two-dimensional water channel, at a specific Reynolds number. The flow visualization is one of the cheap and best techniques which can be used for the visualization of real flow problems.

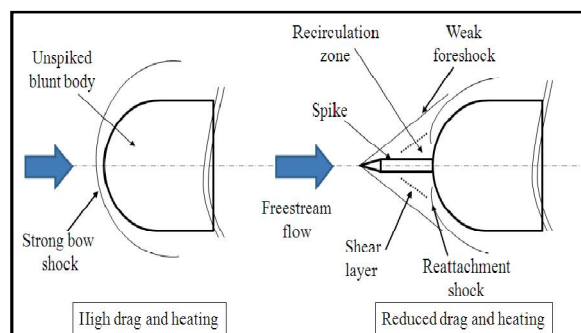


Fig.1 Blunt and Spiked body

International Journal of Innovative Research in Science, Engineering and Technology

(An ISO 3297: 2007 Certified Organization)

Vol. 5, Issue 12, December 2016

II. LITERATURE REVIEW

William H. Bettes et al., [1] the drag coefficient on the road vehicles can be reduced by 24% by changing the front body design shapes and 11% by changing rear body design of the vehicle which accounts for the 25 percent fuel consumption.

Edwin J. Saltzman et al., [2] from their experiments on the rounded corner vehicle of the speed ranging from 30 miles per hour to 65 miles per hour suggested that reduction in aerodynamic drag of about 40 percent can be achieved when compared to the square shaped configuration .

Ashish Vashishtha, et al., [3] studied the comparison between drag on the blunt nosed body with and without breathing nose at the Mach 1.96. The breathing nose is found to reduce the drag on the body by manipulating the high pressure at the nose and the low pressure at the base simultaneously. A maximum drag reduction of 21% was obtained at NPR 2. This is because of the combined effect of the decrease of high pressure at the nose and increase of low pressure at the base, due to the breathing through the nose hole.

E. Rathakrishnan et al., [4] studied the effect of the splitter on the bluff body drag, the body taken is the rectangular cylinder and the studies were carried out for the forward facing splitter plate and backward splitter plate, the results gives for centre line positioning of plate, the backward splitter plate is more effective, whereas for h/4 positioning of plate from the top, the forward plate gives less drag

Khalid M. Sowed et al., [5] study the shielding effect of square-plate and D-shaped front bodies on the drag reduction and the pressure distribution of a three-dimensional bluff body is investigated. The Square-plate front body resulted in maximum of 80% drag reduction. The D-shaped front body was less effective in reducing the drag compared with the square-plate front body

G. K. Suryanarayana et al., [6] reported that the drag of a sphere at high Re can be reduced to more than half its value by passive ventilation from the stagnation region to the base. Simultaneously, the flow field around the base is stabilized and made symmetric, leading to reduction of unsteady aerodynamic forces. The drag of a sphere at high Re can be reduced to more than half its value by passive ventilation from stagnation region to the base. Simultaneously, the flow field around the base is stabilized and made symmetric, leading to reduction of unsteady aerodynamic forces .

Stephen A. Whitmore et al., [7] stated that as for body roughness increases, boundary layer at the model aft thickens and reduces the shearing effect of external flow on the separated flow behind the base region, resulting in reduced base drag. The wind-tunnel tests results conclusively demonstrate the existence of a fore body drag–base drag optimal point. The data demonstrate that the base drag coefficient corresponding to the drag minimum lies between 0.225 and 0.275, referenced to the base area. Most importantly, the data show a drag reduction of approximately 15 percent when the drag optimum is reached.

Shashank Khurana et al., [8] The zone of influence and the positive pressure field over the nose, for a blunt-nosed body, with and without spike, were measured by direct means. Flow past the body, with and without spikes, was visualized in a two-dimensional water channel, at a specific Reynolds number. It is found that, the spike reduces the radius of curvature of the approaching streamline, and the deflection of the streamline is towards the shoulder of the basic body, resulting in a narrow zone of the positive pressure hill at the nose. The spike with hemispherical nose reduces the zone of influence drastically from 1.75 to less than 1.60. The pressure hill height for hemispherical nose is found to be smaller, compared to other shapes of the spike nose studied. The hill heights for the flat faced spike with cylindrical and square stems are comparable. It is found that, the size of the vortex at the junction of the spike and basic body is the largest for the hemispherical nose.

Kalimuthu et al., [9] however, there is no direct address to the magnitude of the positive pressure at the nose and the base pressure at the rear. Also, the recent work of though addressed drag reduction of blunt-nosed body, focuses mainly on reducing the positive pressure at the nose.

V.L. Zhdanov, et al., [10] presented the influence of thin plates and dimples arranged over the upper surface of a coach model on base pressure variations, turbulent wake characteristics, and body drag. The influence of the plate height, the plate spacing, the attack angle, and the distance from the plate trailing edge to the model base on pressure distributions over the model and its back panel are studied. The thin plates only affected by approximately 1% of a total model surface resulted in a 3% reduction of the total body drag. The effect of the dimple array was significantly smaller, and the mechanism of its influence on the shear layer is a subject for further investigation

Sang Joon Lee et. al.[11] studied the effects of installing a small control rod upstream of a circular cylinder experimentally, Control rods with diameters ranging from $d/D = 0.133$ to 0.267 are tested. The drag coefficient of the main circular cylinder decreases about 29% when a control rod of diameter $d = 7$ mm ($d/D = 0.233$) is installed at a pitch ratio close to the critical value of $Lc/D = 2.081$. However, the maximum reduction of the total system drag including that of the control rod (about 25%) is observed at a pitch ratio of $L/D = 1.833$ with a control rod diameter of $d/D = 0.233$.

Yoshio Yajima et al., [12] with their experiments on a circular cylinder with double rows of holes across the diameter with test speed range of $5-9 \times 10^{-3}$ suggested that for medium angles of attack $0^\circ \leq \alpha \leq 60^\circ$ the vortices are more aligned, and consequently the wake region becomes narrower, the pressure difference between the front and rear surfaces of the cylinder is also reduced. Thus a total reduction of 40% of drag coefficient is achieved. This result seems to suggest that the flow around the cylinder with slits with large attack angles is similar to that of a semi-circular arc or semi-circular cylinder, in which the boundary layer separations are fixed at the sharp edges of the arc.

III. EXPERIMENTAL SETUP

In the present study, the flow around a spiked body, comprising of vortices near the stagnation area, was visualized using a rectangular water flow channel. Schematic diagram and a pictorial view of the channel are shown in Figures 3.1(a) and 3.1(b), respectively. Water from the chamber, spills over the inclined plate and is conditioned using an array of wire-meshes, before reaching the downstream of the test-section. The flow quality is found to be fairly uniform in the test-section. The velocity of the flow is measured using the floating-particle method technique, over the length of the test-section. The average of a set of measured velocities is taken as the representative velocity of the flow.

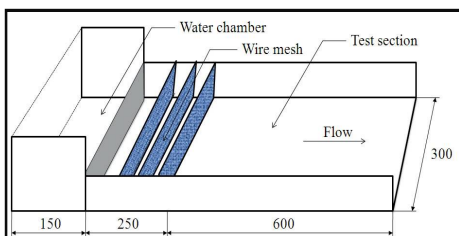


Figure 3.1 (a) Schematic diagram of the experimental set-up (dimensions in mm)

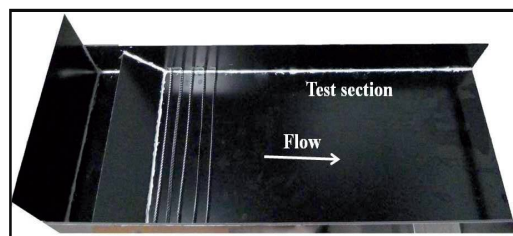


Fig 3.1(b): Pictorial View of the Experimental Set-Up

The schematic diagrams of the test models and spike geometry, in Figure 3.2(a),(b) & (c). The axis of the model was aligned parallel to the flow direction at the middle of test-section for every test. The model consists of a hemisphere-cylindrical fore body with hemispherical spike-nose configurations. W = width of blunt body = 60 mm and L = length of the spike = 90 mm

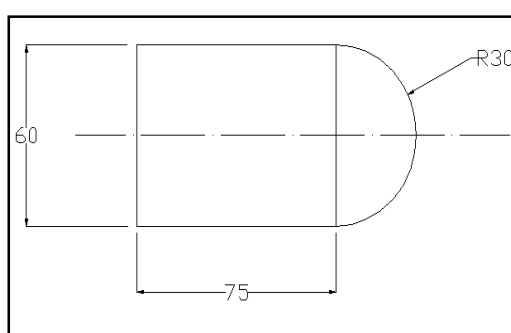


Fig 3.2 (a) Dimensions of basic blunt nosed body

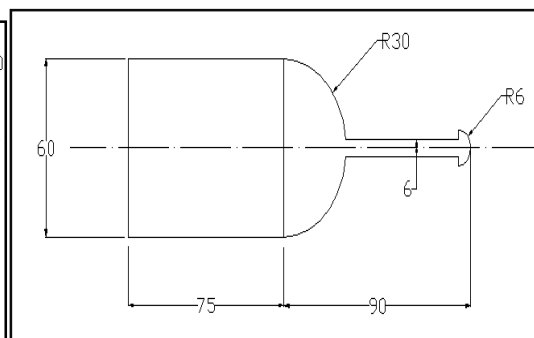


Fig3.2(b) Dimensions of Hemispherical facing spiked blunt body with $L / W = 1$

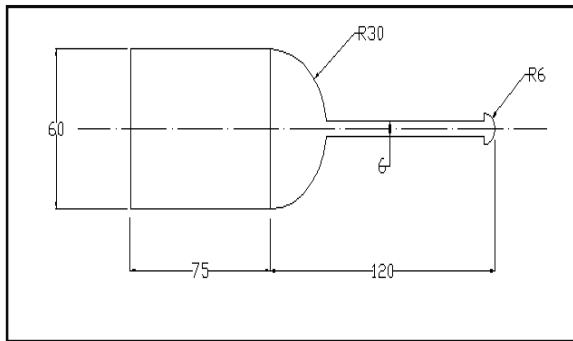


Fig 3.2(c) Dimensions of Hemispherical facing spiked blunt body with $L / W=1.5$

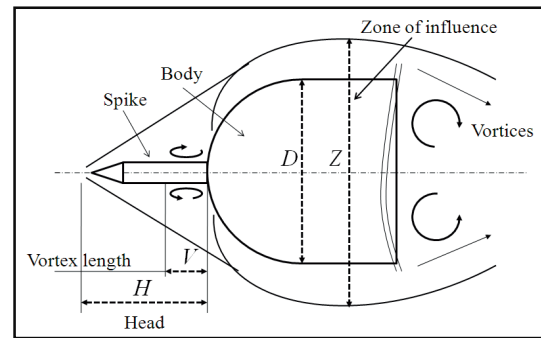


Fig 3.3 Nomenclature of spiked body and geometry

The spiked body nomenclature is shown in above figure 3.3 where H is head also called as length of spike, D is diameter of the blunt body, Z is the Zone of Influence. All the tests of the present study were carried out at Reynolds number 6620 based on the main body diameter. After the proper alignment has been ensured, some time is given for the flow to develop properly. The flow field in the test-section was ensured to be parallel and uniform by observing parallel streak lines of dye injected upstream of the empty test-section. Then the model was placed in the test-section and the flow field was recorded on a video camera. The videos recorded clearly exhibit the zone of influence (Z), head (H) and the vortices (V) at the base.

IV. METHODOLOGY

The specimen is prepared with the help of teak wood with desired shaped with the help of jigsaw machine. The dimensions of the basic specimen is shown in figure 3.2 (a) which looks like a rectangular block is attached with a hemispherical body with a radius of 30mm. Here in the present work the specimen is shown below fig 3.2(b) &(c) which is a modified by providing a spike (projected length) to the basic shape of the body to analyse the drag forces applied on the spiked body.

IV. RESULTS

It is well established that the positive pressure at the nose and the negative pressure at the base, together, causes the large drag associated with blunt nosed bodies meant for high-speed applications. Therefore, it is essential to reduce the positive pressure at the nose and the negative pressure at the base to bring down the drag over the blunt nosed body. In the present investigation with the sole aim of addressing these two parameters, namely the pressure hill (positive pressure zone at the nose) and the zone of influence of the flow field around blunt-nosed body of geometry shown in Figures 3 and 4, with and without spikes, were studied directly using the flow visualization techniques. Some representative visualization pictures of the flow over the body without spike, and with hemispherical spikes, captured in this study, are shown in Figure 5. In the present study the vortex length taken as the distance from the base of the object to the end of the vortex when the reverse flow reaches the model. The length of the vortex is measured with the help of scale calibrated on the test-section and is non-dimensionalised by the width of the model. The vortex length for the model of basic blunt body is about 0.75. This rolling effect behind the object about an edge is called vortex. The low pressure region behind model influences the flow to reverse towards the base. The reverse flow distance is 1.26. The vortex length for the model of hemispherical spike with $L/W=1.5$ is non-dimensionalised with the chord length and it is observed as 0.84. The low pressure region behind model influences the flow to reverse to the base and the reverse flow distance is 1.34. In case of hemispherical spike with $L/W=1$, the vertex length is 1.083 and the low pressure region behind model influence the flow to reverse to the base and the reverse flow distance is non dimensionalised with chord length is 1.34. However, the flow approaches the spike the flow deviates and as it passes over the spike the

International Journal of Innovative Research in Science, Engineering and Technology

(An ISO 3297: 2007 Certified Organization)

Vol. 5, Issue 12, December 2016

recirculation zone forms just behind the spike on both sides. Further, the flow is again reattached to the base model at some place and again recirculation of the flow appears ahead of the base body due which the drag on the blunt nosed body may be reduced due to the effect of spike. The experimental results are shown in below figures 4.1(a),(b) & (c). It is found that the spike reduces the radius of curvature of the approaching streamline, and the deflection of the streamline is towards the shoulder of the basic body resulting in a narrow zone of positive pressure hill at the nose. The spike with hemispherical nose reduces the zone of influence.



Fig 4.1(a) Basic shape of blunt body



Fig 4.1(b) Hemispherical spiked body of $L / W=1.5$.



Fig 4.1(c) Hemispherical spiked body of $L/W=1$

VI. CONCLUSION

The spike of hemispherical configurations attached to the basic blunt nosed body has much influence on the flow field, twin vortex formation and reverse flow distance. There is a considerable increment in the reverse flow distance for model with and without spike. It is observed that the hemispherical spike has given the lowest vortex length compared to the basic blunt nosed body. Whereas coming to the two different configuration of hemispherical spike $L/W=1$ and 1.5 , it is observed that the effect on the flow field is insignificant. It is found that the spike reduces the radius of curvature of the approaching streamline, and the deflection of the streamline is towards the shoulder of the basic body resulting in a narrow zone of positive pressure hill at the nose. The spike with hemispherical nose reduces the zone of influence. So finally it can be concluded that choosing the spike configuration $L/W = 1$ will be beneficial as the economic concern.

REFERENCES

1. William H. Bettes "The aerodynamic drag reduction of road vehicles in earlier" Journal Of Engineering & Science / January 1982
2. Edwin j, Saltman and Robert R. Meyer "drag reduction obtained by rounding vertical corners of box shaped vehicle" NASA Flight research center march 1974.
3. Ashish Vashishtha, Hemant Sharma, P. Lovaraju, and E. Rathakrishnan "Breathing Blunt Nose Concept For Drag Reduction In Supersonic Flow"
4. E. Rathakrishnan "Effect Of Splitter Plate On Bluff Body Drag" Aiaa Journal Vol. 37, No.9, September 1999
5. Khalid M. Sowed and E. Rathakrishnan "Front Body Effects On Drag And Flow Field Of A 3-D Bluff Body" AIAA Journal, VOL.31,NO 7; technical notes

International Journal of Innovative Research in Science, Engineering and Technology

(An ISO 3297: 2007 Certified Organization)

Vol. 5, Issue 12, December 2016

6. G. K. Suryanarayana, Hemming Pauer, G. E. A. Meier "Bluff-Body Drag Reduction By Passive Ventilation" Journal of Experiments in Fluids 16, 73-81 (1993).
7. Stephen A. Whitmore, Stephanie Sprague, Jonathan W. Naughton "Drag Reduction Using Fore Body Surface Roughness" NASA/TM-2001-210390
8. Shashank Khurana, Kojiro Suzuki, Ethirajan Rathakrishnan," Flow Field around a Blunt-nosed Body with Spike, International Journal of Turbo & Jet-Engines, Volume 29, Issue 4, Dec 2012, pp 217-221.
9. R. Kalimuthu and E. Rathakrishnan, Aerodynamic Characteristics of Blunt Nosed Body with and without Aerospikes at Mach 5.87, Proceedings of the 10th Asian Symposium on Visualization, 2010
10. V.L. Zhdanov, H.D. Papenfuss "Bluff Body Drag Control By Boundary Layer Disturbances" Journal of Experiments in Fluids 34 (2003) 460-466
11. Sang-Joon Lee, Sang-Ik Lee, Cheol-Woo Park "Reducing The Drag On A Circular Cylinder By Upstream Installation Of A Small Control Rod" journal of Fluid Dynamics Research 34 (2004) 233-250.
12. Yoshio Yajima, Osamu Sano "A note on the drag reduction of a circular cylinder due to double rows of holes" Journal Of Fluid Dynamics Research 18 (1996) 237-243 .